SPE

Society of Petroleum Engineers of AIME

SPE 8205

A COMPARISON BETWEEN DIFFERENT SKIN AND WELLBORE STORAGE TYPE-CURVES FOR EARLY-TIME TRANSIENT ANALYSIS

by Alain C. Gringarten, Member SPE-AIME, Dominique P. Bourdet, Pierre A. Landel, and Vladimir J. Kniazeff, Member SPE-AIME, FLOPETROL

This paper was presented at the 54th Annual Fall Technical Conference and Exhibition of the Society of Petroleum Engineers of AIME, held in Las Vegas, Nevada, September 23-26, 1979. The material is subject to correction by the author. Permission to copy is restricted to an abstract of not more than 300 words. Write 6200 N. Central Expy., Dallas, Texas 75206.

INTRODUCTION

Well tests have been used for many years for evaluating reservoir characteristics, and numerous methods of interpretation have been proposed in the past. A number of these methods have become very popular, and are usually referred to as "conventional". In the last ten years, many others have been developed, that are often called "modern", but the relationship between "conventional" and "modern" well test interpretation methods is not always clear to the practicing reservoir engineer.

To add to the confusion, some methods have become the subject of much controversy, and conflicting reports have been published on what they can achieve. This is especially true of the "type-curve matching" technique, which was first introduced in the oil literature in 1970[1], for analyzing data from wells with wellbore storage and skin effects. This method, also called "log-log analysis", was supposed to supplement "conventional" techniques with useful qualitative and quantitative information. In recent years, however, it was suggested that this technique be only used in emergency or as a checking device, after more conventional methods have failed.[2,3]

The relationship between "conventional" and "modern" interpretation methods is examined in detail in this paper. It is shown that type-curve matching is a general approach to well test interpretation, but its practical efficiency depends very much on the specific type-curves that are used. This point is illustrated with a new type-curve for wells with wellbore storage and skin, which appears to be more efficient than the ones already available in the literature.

METHODOLOGY OF WELL TEST INTERPRETATION

The Concept of Model

The principles governing the analysis of well tests are more easily understood when one considers well test interpretation as a special pattern recognition problem.

In a well test, a known signal (for instance, the constant withdrawal of reservoir fluid) is applied to an unknown system (the reservoir) and the response of that system (the change in reservoir pressure) is measured during the test.

The purpose of well test interpretation is to *identify* the system, knowing only the input and output signals, and possibly some other reservoir characteristics, such as boundary or initial conditions, shape of drainage area, etc...

This type of problem is known in mathematics as the *inverse problem*. Its solution involves the search of a well-defined theoretical reservoir, whose response to the same input signal is as close as possible to that of the actual reservoir. The response of the theoretical reservoir is computed for specific initial and boundary conditions (direct problem), that must correspond to the actual ones, when they are known.

Interpretation thus relies on models, whose characteristics are assumed to represent the characteristics of the actual reservoir. If the wrong model is selected, then the parameters calculated for the actual reservoir will not be correct.

On the other hand, the solution of the inverse problem is usually not unique : i.e., it is possible to find several reservoir configurations that would yield similar responses to a given input signal. *However, when the number and the range of output signal measurements increase, the number of alternative solutions is greatly reduced.*

For many years, the only models available in the oil literature assumed radial flow in the formation and were only valid for interpreting long term well test data : they were not adequate for analyzing "early-time" data (that is, data obtained before radial flow is established), that were considered as unreliable. The best known and most commonly used

References and illustrations at end of paper

interpretation methods derived from these models are those published by Horner[4] and Miller, Dyes and Hutchinson[5] (MDH), and constitute the so-called "conventional" or "semi-log analysis" techniques.

During the last ten years, much effort has gone into the study of short-time test data, mainly because of the increasingly prohibitive cost of well tests of long duration. Findings (inherent to the inverse problem) can be summarized as follows :

(1) early-time data are meaningful and can be used to obtain unparalleled information on the reservoir around the wellbore.

(2) long-time data are not sufficient for selecting a reservoir model, or, in other words, widely different reservoir models could exhibit the same long-time behavior, thus yielding incorrect or grossly averaged reservoir parameters.

(3) "conventional" methods can be used only for tests of sufficient duration, if and when radial flow is established in the reservoir and boundary effects are not too important.

As a consequence of these studies, a number of new reservoir models have become available, and a more systematic approach to well interpretation can now be used, that provides more reliable analysis results, by taking into account all of the test pressure data (not just those during radial flow).

Futhermore, because of improvements in measuring devices, and the availability of more sophisticated reservoir models, well tests can now provide more information on reservoirs than in the past. Basically, the earlier the test data, the more detailed the reservoir information; or in other words, different ranges of test data yield reservoir parameters characterizing the reservoir behavior on different scales. (This implies that one must know what kind of reservoir information is expected in order to program the test adequately).

This point is best illustrated in Fig. 1. Figure 1 represents a Δp vs Δt log-log plot from a typical test. Δp is the change in pressure since the beginning of the test (taken as positive), and Δt, the time elapsed from the start of the test. The test has been divided into several periods, according to the nature of the information that can be extracted from the corresponding data.

Period $\neq$ 1 corresponds to late-time data and was the first to be investigated by well testing, in the 1920's and 1930's. Production wells were shut-in at regular intervals, and downhole pressure point measurements were taken to obtain the reservoir average pressure, which was then used to estimate the reserves. A material balance (zero-dimensional) model was used for interpretation. As all closed systems have the same pseudo-steady state behavior, no other information can be extracted from such a test.

It was then realized that the validity of these spot pressure measurements was dependent upon the duration of the shut-in period. The less permeable the formation, the longer the shut-in period necessary to reach average reservoir pressure. Transient pressure testing was thus introduced, and was well developed in the 1950's and 1960's. This corresponds to Period $\neq$ 2 on Figure 1. Data from Period $\neq$ 2 are analyzed with "conventional" methods to obtain the permeability-thickness product (kh) of the formation, and the well damage or skin, but these values only represent a gross reservoir behavior. For instance, any horizontal reservoir of infinite extent with impermeable upper and lower boundaries will eventually exhibit radial flow behavior (during the infinite acting Period $\neq$ 2), and the same kh could represent a homogeneous, a multilayered, or a fissured reservoir. In the same way, a negative skin indicates a stimulated well, but data from Period $\neq$ 2 do not permit to decide whether the well was fractured, or simply acidized.

This type of detailed information is only obtained from early time data (Period $\neq$ 3). It is in this time range that, for instance, acidized and fractured wells exhibit different behaviors. Period $\neq$ 3 has been the subject of many studies since the late 1960's, and is the usual target of "modern" (type-curve) analysis.

Type-Curve Analysis

The type-curve approach, however, is very general, and should not be restricted to early time data. Type-curves represent the pressure behavior of theoretical reservoirs with specific features, such as wellbore storage, skin, fractures, etc...

They are usually graphed on log-log paper, as a dimensionless pressure versus a dimensionless time, with each curve being characterized by a dimensionless number that depends upon the specific reservoir model. Dimensionless parameters are defined as the real parameter times a coefficient that includes reservoir characteristics, so that when the appropriate model is being used, real and theoretical pressure versus time curves are identical in shape but translated one with respect to the other, when plotted on identical log-log graphs, with the translation factors for both pressure and time axes being proportional to some reservoir parameters.

Therefore, plotting real data as log-log pressure versus time curves provides qualitative as well as quantitative information on the reservoir. The qualitative information (comparing the shapes of real and theoretical curves) is most useful, for it helps selecting the most appropriate theoretical reservoir model, and breaking down the test into periods with dominating flow regimes, *for which specific analysis methods can be used.*

The type-curve matching method is not new. It was first introduced by Theis[6] in 1935, for interpreting interference tests in aquifers. The availability of new reservoir models, however, has made it particularly powerful for oil and gas well test analysis. In fact, the number of theoretical reservoir models that are actually useful for well test interpretation is limited, and these theoretical reservoir models exhibit specific features that are easily recognizable on a log-log graph. For example, wellbore storage yields a log-log straight line of slope unity at early times (Δp is proportional to Δt)[1] whereas an infinite conductivity fracture yields a log-log straight line with half-unit slope (Δp is proportional to $\sqrt{\Delta t}$) . In the same way, a finite

conductivity fracture was found to yield a one-fourth unit slope straight line (Δp is proportional to $\sqrt[4]{\Delta t}$)[8]. Radial flow (Δp proportional to log Δt)[9]; spherical flow (Δp proportional to $1/\sqrt{\Delta t}$)[10] and pseudo-steady flow (Δp, linear function of Δt)[11] also exhibit distinctive log-log shapes.

However, for the analysis to be correct, all of the features of the theoretical model must be found in the actual well test data, and all results from specific analysis methods implied by the model must be consistent. Specifically, if, for instance, wellbore storage is present, all the points on the unit slope log-log straight line must also be located on a straight line passing through the origin when Δp is plotted versus Δt in cartesian coordinates, and vice-versa. Similarly, in the case of a vertical fracture of infinite conductivity, the points on the half-unit slope log-log straight line must line up in a Δp vs $\sqrt{\Delta t}$ cartesian plot. The same applies to all other flow regimes, and, in particular, *the proper semi-log straight line used in "conventional" analysis methods exists only for the points that exhibit the radial flow typical shape on the log-log plot.*

Two types of plot are therefore useful in well test interpretation :

(1) a log-log plot of *all test data*, which is used to identify the various flow regimes, and to select the most appropriate reservoir model (Diagnostic Plot). Such a plot should be made prior to any analysis, provided, of course, that the necessary data are available (namely, the time and pressure at the start of the test);

and (2) specialized plots as needed, that are specific to each flow regime identified on the log-log plot (Δp vs Δt, Δp vs $\sqrt{\Delta t}$, Δp vs $\sqrt[4]{\Delta t}$, Δp vs log Δt, etc...), and only concern *appropriate segments* of the test data.

In order to provide quantitative reservoir information, the log-log plot of the test data must be matched against a type-curve from a theoretical model that includes the various features identified on the actual data. For a given theoretical model, however, not all type-curves are equivalent. Depending upon the choice of dimensionless pressure and time parameters, one type-curve may be easier to use within a specific data range, and different graphs of the same type-curve data are common in the literature. For instance, the dimensionless pressure for an infinite conductivity vertical fracture,

$$p_D = \frac{kh}{141.2qB\mu}\Delta p \qquad (1)$$ ★

was graphed versus

$$t_{DA} = \frac{0.000264kt}{\phi\mu c_t A} \qquad (2)$$

in Ref. 12, and versus

$$t_{Df} = \frac{0.000264kt}{\phi\mu c_t x_f^2} = t_{DA}\left(\frac{A}{x_f^2}\right) \qquad (3)$$

in Ref. 7. In Eq. 3, A represents the drainage area, and x_f, the half fracture length. The former plot is better suited for late time analysis, whereas the latter is more efficient for early time analysis.

In the same way, the type-curve for a horizontally fractured well was first presented in terms of p_D (Eq. 1) versus

$$t'_{D_f} = \frac{0.000264kt}{\phi\mu c_t r_f^2} \qquad (4)$$

where r_f is the fracture radius, then as

$$\frac{p_D}{h_D} = \frac{\sqrt{k_r k_z}\, r_f \Delta p}{141.2qB\mu} \qquad (5)$$

versus the same t'_{Df}[7].

Another example concerns the finite conductivity vertical fracture, for which a first type-curve[14] was produced as p_D (Eq. 1) versus t_{Df} (Eq. 3). This type-curve was subsequently redrafted as[8] :

$$\left[p_D\, k_{fD}\, w_{fD}\right] \quad \text{vs} \quad \left[t_{Df}\left(k_{fD}\, w_{fD}\right)^2\right]$$

where

$$k_{fD}\, w_{fD} = \frac{k_f w}{k x_f} \qquad (6)$$

represents the dimensionless fracture conductivity. Another useful presentation would be in terms of p_D (Eq. 1) versus

$$t_{De} = \frac{0.000264\ kt}{\phi\mu c_t r_{we}^2} \qquad (7)$$

where r_{we} is an effective wellbore radius[15], that depends upon the fracture conductivity ($r_{we}=\frac{x_f}{2}$ for an infinite conductivity vertical fracture).

In general, type-curve matching is easier when all the theoretical curves on the type-curve graph merge into one single curve where the actual well data are the most numerous (dominating flow regime). Another important requirement is that the various flow regimes be clearly indicated, with limits computed from realistic approximation criteria, so that appropriate specific analysis methods can be applied to the corresponding test data. This last point is particularly important, as specific analysis methods, that use the slope of the straight line on the specialized plots, provide usually more accurate results than quantitative log-log analysis.

In the following, we present a new type-curve for wells with wellbore storage and skin effects, that was developed according to the above rules. This type-curve has been used for the analysis of many well tests, and was found to be more efficient than the ones already published in the literature.

★ Oil field units are used in the formulae.

PUBLISHED WELLBORE STORAGE AND SKIN TYPE-CURVES

A number of type-curves for wells with wellbore storage and skin effects have been published at various times in the past. They are reviewed in Ref. 3. We will only consider here the three that are most commonly used in well test analysis.

Agarwal, Al-Hussainy, and Ramey (Ref. 16)

The type-curve published by Agarwal, et al.[16] is shown in Fig. 2. The dimensionless pressure, p_D (from Eq. 1), on the y-axis, is plotted versus a dimensionless time :

$$t_D = \frac{0.000264kt}{\phi\mu c_t r_w^2} \qquad (8)$$

on the x-axis. Each curve corresponds to a specific value of the skin S and the dimensionless wellbore storage parameter :

$$C_D = \frac{0.8936\ C}{\phi c_t h r_w^2} \qquad (9)$$

where C is the wellbore storage constant.

The curves were computed from an analytical solution to the diffusivity equation representing the constant rate drawdown in a finite radius well with an infinitesimal skin in an infinite reservoir. The solution was first obtained in the Laplace domain, as :

$$L\{p_D\} = \frac{K_0(\sqrt{p}) + S\sqrt{p}\,K_1(\sqrt{p})}{p\{\sqrt{p}\,K_1(\sqrt{p}) + C_D\,p[K_0(\sqrt{p}) + S\sqrt{p}\,K_1(\sqrt{p})]\}} \qquad (10)$$

where K_0 and K_1 are the modified Bessel functions of the second kind of zero and unit orders, and p the Laplace parameter.

Inversion of Eq. 10 by means of Mellin's formula was obtained as :

$$p_D = \frac{4}{\pi^2}\int_0^\infty \frac{\left(1 - e^{-u^2 t_D}\right) du}{u^3\left\{\left[u\,C_D\,J_0(u) - (1 - C_D S u^2)J_1(u)\right]^2 + \left[u\,C_D\,Y_0(u) - (1 - C_D\,Su^2)Y_1(u)\right]^2\right\}} \qquad (11)$$

where J_n and Y_n are the Bessel functions of the first and second kind of n^{th} order, respectively.

Eq. 11 was used for positive skin calculations. The negative skin situation was approximated by evaluating Eq. 11 at S = 0, but for dimensionless time and storage constants based on the effective wellbore radius, $r_w e^{-S}$ (respectively, $t_D e^{2S}$ and $C_D e^{2S}$), S being the actual negative skin value.

As mentioned earlier, wellbore storage effects ($C_D \neq 0$) are characterized by a unit slope log-log straight line; the $C_D = 0$ curves do not exhibit such behavior. The time when radial flow starts approximately corresponds to the intersection of $C_D = 0$ and $C_D \neq 0$ curves, for appropriate C_D and S values. The semi-log radial flow approximation (used in "conventional" analysis) is only valid for pressure points beyond that intersection.

Efficient use of this type-curve requires C_D to be known for the well of interest. If this is the case, well test data can be matched easily with one of the theoretical curves corresponding to this C_D value, thus yielding the skin S. The kh product can then be computed from the pressure match. The time match is not usually used, because of uncertainty on the effective radius . If "conventional" methods are applicable, they should yield a kh value consistent with that of the pressure match.

On the other hand, if C_D cannot be evaluated, matching becomes rather difficult, different C_D,S curves having similar shapes. One can then only estimate the start of the semi-log straight line (if sufficient test data).

McKinley (Ref. 17)

McKinley's type-curve is shown in Fig. 3. Contrary to Agarwal, et al.'s, this type-curve was prepared for build-up analysis. The shut-in time, in minutes, is the ordinate, with a pressure build-up group, equal to $\frac{5.61\ C\ \Delta p}{Bq}$, in days, plotted along the abscissa. Each curve is for a constant value of transmissivity group, $\frac{kh}{5.61\mu C}$, in $\frac{md.ft.psi}{bbl.cp}$.

McKinley's type-curve was computed numerically, with a finite difference model. After the time at which wellbore storage disappears, each curve was calculated with the exponential integral (line source) function for a time corresponding to about 0.2 of a log cycle on a standard semi-log plot, then drawn so as to approach asymptotically pressure group values for a circular reservoir with a drainage radius $r_e = 2000\ r_w$.

All calculations were made for zero skin, and a single value of the diffusivity group

$$\frac{k}{\phi\mu c_t r_w^2} = 10^7\ \frac{md\ psi}{cp\ sqft}$$

, on the basis that this group was much less influential on the pressure response than the transmissivity group.

Test data, with Δt in minutes on the y-axis and Δp, in psi on the x-axis, are matched with the type-curve by first adjusting the y-axis, and then moving the data graph parallel to the x-axis until a good fit is obtained. A good match of all the data points is indicative of a well without significant damage or stimulation. On the other hand, if the last data points trend toward the left of the

curve, the well is likely to be damaged. It is stimulated if the trend is toward the right.

The transmissivity of the formation around the wellbore is calculated from the curve and the x-axis (pressure group) match. If the well is not damaged nor stimulated, this value also represents the transmissivity of the formation away from the wellbore. If the well is damaged or stimulated, the transmissivity away from the wellbore can be evaluated by matching the last data points with one of the curves on the left, or on the right, respectively, of the initial match.

Earlougher and Kersch (Ref. 2)

Earlougher and Kersch's drawdown type-curve is presented in Fig. 4. Each curve is plotted as :

$$\frac{\Delta p}{\Delta t}\frac{24C}{qB} = \frac{p_D C_D}{t_D} \quad \text{versus}$$

$$\frac{kh}{\mu}\frac{\Delta t}{C}, \quad \frac{md.ft}{cp} \cdot \frac{hr}{bbl/psi} = \frac{1}{0.000295}\frac{t_D}{c_D}$$

for a given value of $C_D e^{2S}$.

This type-curve is, in fact, the same as that of Agarwal, et al.'s, and was computed from Eq. 11. Its presentation, of course, is very different because of the choice of the dimensionless parameters.

These are based on the effective wellbore radius, $r_w e^{-S}$, so that the various families of curves in Fig. 2, corresponding to different C_D and S values, are reduced into one single family of curves characterized by $C_D e^{2S}$. This approximation is exact at very early times, when wellbore storage effects dominate $\left(p_D = \frac{t_D}{C_D}\right)$, and at long times, after the radial flow log approximation applies. It is reasonably accurate at intermediate times.

One interesting feature of Earlougher and Kersch's type-curve is that all curves are asymptotical to $\frac{p_D C_D}{t_D} = 1$, at early times (because of the wellbore storage flow equation). This corresponds to an asymptote of the real data ratio $\frac{\Delta p}{\Delta t}$, equal to $\frac{qB}{24C}$. If C can be evaluated (from completion data or, best, from either the log-log unit slope straight line or the early time data Δp versus Δt plot), this asymptote may be used to position a plot of $\frac{\Delta p}{\Delta t}$ versus Δt on the type-curve, so that matching can be performed with horizontal sliding only, as with the McKinley curve. The permeability-thickness product is then obtained from the time match, and $C_D e^{2S}$ from the curve match, which will yield S if C_D is known.

The main limitation of the type-curve concerns the lack of information on the limits of the various flow regimes (the same remark applies to the McKinley type-curve). Another problem is that it requires specific computation of $\frac{\Delta p}{\Delta t}$ which may appear combersome.

NEW WELLBORE STORAGE AND SKIN TYPE-CURVE

Drawdown Analysis

A new-type curve is presented in Fig. 5. This type-curve is given as p_D (from Eq. 1) versus $\frac{t_D}{C_D}$, each curve being characterized by a value of $C_D e^{2S}$.*

The limits of the various flow regimes (end of storage, and start of semi-log radial flow) shown on the type-curve correspond to a 5% approximation, percentage that was found to be well suited for practical applications. Also indicated are the ranges of $C_D e^{2S}$ for various well conditions (damaged, zero-skin, acidized, and fractured). All curves (except for very low $C_D e^{2S}$ values) merge into a single unit straight line at early times, when wellbore storage effects dominate. The axis on the right is for build-up analysis and will be discussed later.

This type-curve is used in the usual manner : the test data are plotted as Δp versus Δt on a log-log graph of the same size as that of the type-curve, and matched with one of the curves. When wellbore storage is present, matching can be made more conveniently by first overlaying the initial unit slope straight lines on both (test data and type-curve) graphs, and then sliding the data graph along this 45° direction until the best match is obtained. This yields a value for $C_D e^{2S}$, and for S if C_D is known.

The permeability thickness product can be calculated from the pressure match *or* from the time match (when a value of the storage constant is available). Of course, results should be identical. One important point is that only kh can be obtained from axis match, as with Earlougher and Kersch's type-curve; and not $\phi c_t h$, as Agarwal et al.'s presentation would seem to imply (although, as mentioned before, the time match is rarely used with the type-curve of Fig. 2). Alternatively, the time match can be used to compute the wellbore storage constant.

The basic model used to construct the type-curve of Fig. 5 is identical to that of Agarwal et al.[16]'s, namely a finite radius well with an infinitesimal skin and wellbore storage, in an infinite reservoir. There are some fundamental differences, however.

Contrary to what was stated in Ref. 16, Eq. 10 cannot be inverted for negative skins. The use of an infinitesimal negative skin at the sand face would imply generation of energy in the porous medium, and yield instability in the flow equation. The only way to simulate a negative skin is to assume infinite conductivity up to an effective radius $r_{we} = r_w e^{-S}$ as was indeed done in Ref. 16, but there is a lower limit in terms of $C_D e^{2S}$. This can be shown by the following simple calculation : if we assume that the zone of infinite conductivity around the well has the same porosity as the formation, the corresponding wellbore storage constant is equal to :

* Large-scale copies of Fig. 5 are available from the authors upon request.

$$C_S = C + \pi\left(r_{we}^2 - r_w^2\right)h\phi c_t \quad (12)$$

where C is the real wellbore storage constant. The resulting dimensionless wellbore storage constant is thus :

$$\left(C_D\right)_S = C_D e^{2S} = \left(C_D e^{2S}\right)_w + \frac{1 - e^{2S}}{2} = C_D\, 0.5 \quad (13)$$

The smallest possible value for $C_D e^{2S}$ is 0.5. *Lower values of $C_D e^{2S}$ must correspond to fractured wells with wellbore storage.* In the type-curve of Fig. 5, these were obtained for a well with an infinite conductivity vertical fracture, as in Ref. 18. Actual computations were made with a wellbore storage simulator[15]. The S in the $C_D e^{2S}$ group, for $C_D e^{2S} < 0.5$, represents an equivalent skin based upon the effective radius $r_{we} = x_f/2$:

$$S = S_f = \ln \frac{r_w}{r_{we}} \quad (14)$$

The following relationship holds :

$$C_D e^{2S_f} = \left(\frac{x_f}{r_{we}}\right)^2 \qquad C_{Df} = 4\, C_{Df} \quad (15)$$

where C_{Df} is the fractured well dimensionless wellbore storage coefficient defined in Ref. 18 :

$$C_{Df} = \frac{0.8926\, C}{\phi c_t\, h\, x_f^2} \quad (16)$$

All curves corresponding to $C_D e^{2S} \geq 0.5$ were computed by evaluating Eq. 11 at S = 0, but for dimensionless time and storage constants based on the effective wellbore radius, $r_w e^{-S}$ (respectively, $t_D e^{2S}$ and $C_D e^{2S}$), as was done by Agarwal, et al.[16] for negative skins, and by Earlougher and Kersch[2] for positive skins. In order to verify that $C_D e^{2S}$ was indeed the governing parameter, Eq. 11 was also evaluated, for a given $C_D e^{2S}$ value, with fixed values of C_D (10^2, 10^3, 10^4 and 10^5) and the corresponding S (for positive skins only). The difference between the various S = 0 and S ≠ 0 curves was less than 0.1% for all the $C_D e^{2S}$ values (10^3, 10^4, 10^6, 10^8, 10^{10}, 10^{15}, 10^{20}, 10^{30}) that were investigated.

Time limits for the different flow regimes were evaluated from the difference, for a given $C_D e^{2S}$ value, between the p_D value from Eq. 11, and that from the appropriate approximation equation, namely :

$$p_D = \frac{t_D}{C_D} \quad (17)$$

for storage flow[1], and :

$$p_D = \frac{1}{2}\left(\ln \frac{t_D}{C_D} + 0.80907 + \ln C_D e^{2S}\right) \quad (18)$$

for radial flow.

Fig. 6 gives the dimensionless time, $\frac{t_D}{C_D}$, at the end of the log-log unit slope straight line (wellbore storage) for various percentage differences between p_D from Eq. 11 and p_D from Eq. 17. As mentioned before, the 5% difference curve seems best suited for practical applications. The various curves of Fig. 6 can be approximated with reasonable accuracy (within 5%) by :

$$\frac{t_D}{C_D} = \alpha \ln\left[3\alpha\, C_D e^{2S}\right] \quad , \; C_D e^{2S} > 10^3 \quad (19)$$

α being the percentage difference (0.01 for 1%, 0.05 for 5%, and 0.10 for 10%). Related equations proposed by Agarwal, et al[16]. :

$$\frac{t_D}{C_D} = 0.2S, \text{ for } S \neq 0 \quad \text{and} \quad \frac{t_D}{C_D} = 0.4 \text{ for } S = 0 \quad (20)$$

correspond approximately to a 8% difference between Eqs 11 and 17.

Starting times for the radial flow semi-log approximation are presented in Fig. 7, for various percentage differences between Eqs 11 and 18 (0.1, 0.5, 1,5 and 10%). For a given percentage difference, the semi-log approximation becomes valid at an earlier time for acidized wells, and at a later time for fractured wells, as compared with wells with zero or positive skins. Again, a 5% difference appears to be appropriate for well test analysis.

Also included in Fig. 7 are starting time curves derived from various criteria published in the literature. The "one and one half log cycle" rule[3] , which states that the start of the semi-log straight line occurs on a log-log graph about 1 1/2 log cycles after the end of the unit slope straight line, is reasonably good for damaged wells ($C_D e^{2S} > 10^6$). The percentage figures on the curves refer to the end of the unit slope straight line, as defined in the previous paragraph.

Ramey, et al.[20]'s formula :

$$t_D = C_D\,(60 + 3.5S) \quad (21)$$

also gives accurate results for damaged wells ($C_D e^{2S} > 10^3$). It approximately corresponds to a 2% difference between Eqs 11 and 18. On the other hand, the equation proposed by Chen and Brigham[21]:

$$t_D = 50\, C_D \exp(0.14S) \quad (22)$$

yields time limits that are very different from the ones found in this paper, or those obtained from either Eq. 21 or the "one and one half log cycle" rule. The fact that Eq. 22 was derived from build-up type-curves is not sufficient for justifying such discrepancy, as will be seen in the following chapter.

Build-Up Analysis

It has been pointed out[1] that build-up data could be analyzed with drawdown type-curves, by using the difference between the pressure during the test, and the pressure at the start of the test, provided that the producing time was much greater than the longest shut-in time (10 times greater was suggested as a rule of thumb).

The effect of the producing time was recently investigated by Raghavan[22] , who produced a number of build-up type-curves, with the dimensionless build-up pressure

$$\left(p_D\right)_s = \frac{kh}{141.2qB\mu}\left[p_{ws}(\Delta t) - p_{ws}\,(\Delta t = 0)\right]$$

$$= p_D\,(\Delta t) + p_D\left(t_p\right) - p_D\left(t_p + \Delta t\right) \quad (23)$$

plotted as a function of the dimensionless shut-in time, Δt_D (from Eq. 8). p_{ws} is the shut-in pressure

t_p the production time, and $p_D(t)$ the dimensionless drawdown pressure function of Agarwal et al.[16] Raghavan concluded from his study that, for practical purposes, the drawdown solutions could be used for log-log analysis of build-up data when :

$$t_D/C_D \geq 50 \qquad (24)$$

In mathematical terms, this is equivalent to approximating Eq. 23 by :

$$(p_D)_s = p_D\,(\Delta t) \qquad (25)$$

Surprisingly, no condition was placed on the duration of the build-up.

Our conclusions are different. We present in Fig. 8 build-up type-curves obtained by using Eq. 23 with p_D's from Fig. 5 and corresponding to producing times, $\frac{t_p}{C_D}_D$, equal to 10^2, 5.10^2, 10^3, 5.10^3 and 10^4. It can be seen that these differ at long times from the drawdown type-curves for all C_De^{2S} values shown on the graph. The thin dotted lines correspond to points on the drawdown curves where there is a 5% difference between drawdown and build-up, for a given production time. It is apparent that, the greater the damage, the shorter the length of the production period required for analyzing build-up data with drawdown type-curves.

This result is illustrated in Fig. 9. Fig. 9 shows the pressures on the drawdown curves where there is a 1% and 5% difference between drawdown and build-up, as a function of the ratio $\Delta t/t_p$. A single curve is obtained for most production times. It is obvious from Fig. 9 that $\frac{\Delta t}{t_p}$ varies greatly and can be greater than unity for high p_D's (i.e. high C_De^{2S} values). $\frac{\Delta t}{t_p} = 0.1$ would correspond to slightly damaged or stimulated wells, if the 1% difference curve is used, and to fractured wells with the 5% difference curve.

The fact that, for damaged wells, drawdown type-curves can be used for analyzing shut-in pressures even if the longest build-up time is large compared to the production time, is obvious from Eq. 23. Eq. 23 can be approximated by Eq. 25 when :

$$p_D(t_p) - p_D\,(t_p + \Delta t) \ll p_D\,(\Delta t) \qquad (26)$$

which is achieved, either when Δt is small compared to t_p[1], *or* when the p_D function is large and exhibits little variation over a wide time range, as in the case of high C_De^{2S} values.

The 5% difference curve of Fig. 9 was used for preparing the $\Delta t/t_p$ axis on the right hand side of Fig. 5, whose purpose is to check the validity of matching build-up data on the drawdown type-curve. This is done in the following manner : the $\Delta t/t_p$ ratio for the last build-up point matched on a drawdown curve is used to compute the minimum duration of the production period for that match to be valid; if the actual drawdown duration is greater than this minimum value, the match is likely to be correct. If, on the other hand, the actual drawdown duration is smaller, the build-up curve corresponds to a lower C_De^{2S} value, and a new match should be attempted. In the new match, the point under consideration should fall below the drawdown type-curve.

Checking the validity of the build-up match is a very important step in build-up log-log analysis. Failure to do so may result in a match with a drawdown curve corresponding to a C_De^{2S} that is too high, thus giving a permeability-thickness product greater than the actual value. If semi-log analysis is applicable, a MDH plot will also yield too high a kh, which may be consistent with that from log-log analysis, thus giving the false impression of correct interpretation results. A Horner plot, on the other hand, will yield the correct answer, provided an appropriate production time is used.

This possibility of obtaining different results from MDH and Horner analysis when the semi-log approximation is valid for the build-up has been mentioned in the literature [3, 12, 21, 22, 23] but the reason for it has not been clearly stated. In fact, the real relationship between the MDH and the Horner methods seems to have been largely overlooked. The Miller-Dyes-Hutchinson method is usually presented as a limiting case of the Horner method, when Δt is very small compared to t_p. This happens to be a particular case. The MDH and the Horner techniques are two different methods of interpretation.

The MDH plot is actually a "specialized" plot associated with log-log analysis and corresponds to the semi-log approximation of Eq. 25 for build-up data. As discussed in the introduction of this paper, Eq. 25 also implies that the *matched data* can be analyzed by methods specific to the various flow regimes identified on the type-curve. In the particular case of the wellbore storage and skin type-curve of Fig. 5, storage flow yields a straight line on a $p_{ws}\,(\Delta t) - p_{ws}\,(\Delta t = 0)$ vs Δt cartesian plot, from which the wellbore storage constant can be evaluated. In the same way, a straight line with slope proportional to kh is obtained when $p_{ws}\,(\Delta t) - p_{ws}\,(\Delta t = 0)$ is plotted versus log Δt, after the semi-log approximation becomes valid. This last plot is *the* MDH plot. It can be used only when type-curve matching is applicable, i.e. when the production period has the proper minimum duration, as indicated on Fig. 5. If departure from the drawdown type-curve occurs before the log approximation becomes valid on the specific drawdown curve being matched, the MDH plot cannot be used.

In such a case, on the other hand, a Horner plot will yield correct kh values. The general equation corresponding to Horner analysis is :

$$\frac{kh}{141.2qB\mu}\left[p_i - p_{ws}\,(\Delta t)\right] = p_D\left(t_p + \Delta t\right) - p_D(\Delta t) \qquad (27)$$

If the semi-log approximation applies to the drawdown type-curve at Δt, it also applies at $t_p + \Delta t$, whatever the value of the t_p may be, provided there is no overhelming boundary effects. Eq. 27 takes the classical form :

$$\frac{kh}{141.2qB\mu}\left[p_i - p\,(\Delta t)\right] = 1.151 \log \frac{t_p + \Delta t}{\Delta t} \qquad (28)$$

Another possibility for analyzing build-up data consists in plotting :

$$p_{ws}\,(\Delta t) - p_{wf,ext}\,(\Delta t) \quad \text{vs} \quad \Delta t$$

where $p_{wf,ext}$ is the drawdown pressure extrapolated

at a shut-in time Δt, i.e. corresponding to a production time equal to $t_p + \Delta t$. Because :

$$\frac{kh}{141.2qB\mu}\left[p_{ws}(\Delta t) - p_{wf,ext}(\Delta t)\right] = p_D(\Delta t) \quad (29)$$

at all times, such a plot will match the drawdown type-curve, without restrictions on Δt or t_p. When the semi-log approximation applies, a Horner plot and a MDH plot of $[p_{ws}(\Delta t) - p_{wf,ext}(\Delta t)]$ vs log Δt will yield the same kh.

This method of analysis is well known in hydrogeology, and has been mentioned several times in the oil literature.[22,24,25] It is more convenient for build-up log-log analysis that the method discussed previously $[p_{ws} - p_{ws}(\Delta t = 0)$ vs $\Delta t]$, but requires a good estimate of the extrapolated drawdown pressure.

Multiple Rate Analysis

Most of the remarks that were made in the previous chapter on build-up analysis, apply to multiple rate analysis. "Build-up" must be replaced by "actual flow sequence" and "Drawdown" by "previous flow sequence", except in "drawdown type-curve", where it refers to the first flow sequence in the series, after stabilization.

Assuming n subsequent flow sequences, each one with a rate q_i (≥ 0) and a duration Δt_i, Eq. 23 becomes :

$$(p_D)_S = \frac{kh}{141.2(q_{n-1} - q_n)B\mu}\left[p_{ws}(\Delta t) - p_{ws}(\Delta t = 0)\right]$$

$$= \frac{q_1}{q_{n-1} - q_n}\left[p_D\left(\sum_{i=1}^{n-1}\Delta t_i\right) - p_D\left(\sum_{n=1}^{n-1}\Delta t_i + \Delta t\right)\right]$$

$$+ \frac{q_2 - q_1}{q_{n-1} - q_n}\left[p_D\left(\sum_{i=2}^{n-1}\Delta t_i\right) - p_D\left(\sum_{i=2}^{n-1}\Delta t_i + \Delta t\right)\right]$$

$$+ \ldots$$

$$+ \frac{q_{n-1} - q_{n-2}}{q_{n-1} - q_n}\left[p_D(\Delta t_{n-1}) - p_D(\Delta t_{n-1} + \Delta t)\right] + p_D(\Delta t) \quad (30)$$

where Δt is the time elapsed in the actual (n^{th}) flow sequence. As in the build-up analysis, log-log analysis with drawdown type-curves is possible if (1) Δt is small compared to Δt_{n-1}, the duration of the *previous* flow period, or (2) each term on the right hand side of Eq 30, (but the last) is negligible with respect to $p_D(\Delta t)$. With the type-curves of Fig. 5, this is achieved as soon as $(\Delta t_{n-1})_D/C_D$ is greater than 100 for high C_De^{2S} values. The $\Delta t/t_p$ axis on the right hand side of Fig. 5 can be used for checking the validity of the log-log analysis, with $t_p = \Delta t_{n-1}$. Restrictions on the use of the MDH plot are the same as in build-up analysis.

On the other hand, log-log analysis with drawdown type-curves is always possible with a log-log plot of $[p_{w,n}(\Delta t) - p_{w,n-1,ext}(\Delta t)]$ versus Δt, where $p_{w,n}$ is the pressure in the flow sequence being analyzed, and $p_{w,n-1,ext}$ the extrapolated pressure corresponding to the previous flow period. The multiple rate analog of Eq. 29 is :

$$\frac{kh}{141.2(q_{n-1} - q_n)B\mu}\left[p_{w,n}(\Delta t) - p_{w,n-1,ext}(\Delta t)\right] = p_D(\Delta t) \quad (31)$$

In the same way, the Horner formula in Eq. 27 becomes :

$$\frac{kh}{141.2(q_{n-1} - q_n)B\mu}\left[p_i - p_{w,n}(\Delta t)\right] =$$

$$\frac{q_1}{q_{n-1} - q_n}p_D\left(\sum_{n=1}^{n-1}\Delta t_i + \Delta t\right) + \frac{q_2 - q_1}{q_{n-1} - q_n}p_D\left(\sum_{n=2}^{n-1}\Delta t_i = \Delta t\right)$$

$$+ \frac{q_3 - q_2}{q_{n-1} - q_n}p_D\left(\sum_{n=3}^{n-1}\Delta t_i + \Delta t\right) + \ldots - p_D(\Delta t) \quad (32)$$

In order for the usual superposition method to be applicable, it is only necessary that the semi-log approximation be valid for $p_D(\Delta t)$, provided, of course, that no significant boundary effects exist for the other terms. The rates for each flow sequence must be known, however, for applying Eq. 32.

COMPARISON BETWEEN TYPE-CURVES

The type-curve presented in this paper is compared in Figs 10 to 13 with the ones shown in Figs 2 to 4, redrafted as p_D vs $\frac{t_D}{C_D}$.

Excellent agreement is found in Fig. 10 with the type-curve of Agarwal, et al.[16], and in Fig. 12 with that of Earlougher and Kersch[2]. This was to be expected, as the same mathematical model and analytical formulae were used. The type-curves should thus yield similar analysis results if properly used within their validity range. Earlougher and Kersch type-curve of Fig. 4 can in fact be matched with that of Fig. 5 by means of a 45° counterclockwise rotation, but they do not include negative skins. It must be noted also that Agarwal, et al.'s[16] curves are slightly different from ours for strongly stimulated wells, since we used the infinite conductivity vertical fracture solution. The thick dotted line in Fig. 10 corresponds to the start of the semi-log straight line as evaluated visually from the intersection of $C_D = 0$ and $C_D \neq 0$ curves in Fig. 2. It corresponds to Eq. 22, with a smaller precision.

Fig. 11 shows the comparison with the McKinley[17] build-up type-curve. It can be seen that all the curves of Fig. 3 fall in the zero skin region of the type-curve presented in this paper. However, for $\frac{t_D}{C_D}$ greater than 100, after the semi-log approximation becomes valid within 1%, the McKinley curves become horizontal. This corresponds to constant pressure boundary effects, that were included in the model. It is not due to insufficient production time. The transition between radial flow and constant boundary pressure at $r_e = 2000r_w$ is only approximate[27], but this should not affect early time analysis of tests in wells without significant damage or stimulation. However, the existence of boundaries in the type-curve model must be kept in mind

when a "reservoir" match is attempted with data from a stimulated or damaged well.

The last comparison shown on Fig. 13 concerns the type-curve for finite conductivity vertical fractures with wellbore storage, published by Cinco and Samaniego[19]. C_r is the dimensionless fracture conductivity, equal to $\frac{1}{\pi}$ times the term on the right end side of Eq. 6. S_f and C_{Df} are given by Eqs 14 and 16, respectively. r_{we} is obtained as a function of C_r from Fig. 9 of Ref. 14. All the curves from Ref. 19 shown in Fig. 13 correspond to C_De^{2S}'s values between 4 and 6.10^{-3}. They are in good agreement with the corresponding C_De^{2S} curves in Fig. 5 at long times (after the semi-log approximation becomes valid), and at very early times, during storage flow. At intermediate times, however, they differ greatly. This example illustrates well what was pointed out in the beginning of the paper : data from a specific time range cannot be used to predict the system behavior in a later time range, unless additional knowledge on the well is available. Analyzing finite conductivity early time data with an infinite conductivity model should yield erroneous results.

EXAMPLE ANALYSIS

The use of the type-curve presented in this paper is illustrated with the test following acidification on a new well shown on Fig. 14. Pertinent reservoir and pressure data are given in Table 1.

A log-log plot of the test data is presented in Fig. 15. As the initial pressure was not available, log-log analysis was first attempted with build-up data graphed as $[p_{ws}(\Delta t) - p_{ws}(\Delta t = 0)]$ vs Δt (circles in Fig. 15). A good match, not shown, was obtained with all the data points falling on the $C_De^{2S} = 10$ curve indicating no or little stimulation, and the start of the semi-log straight line at $\Delta t = 5.5$ hrs. Selecting a match point :

$$p_D = 0.29;\ \frac{t_D}{C_D} = 0.48 \Big/ p_{ws} - p_{ws}(\Delta t=0)=10\text{psi};\ \Delta t = 0.1\text{hr}$$

and using the pressure match for computing kh yields :

$$kh = 141.2qB\mu\left(\frac{p_D}{\Delta p}\right)_{match} =$$

$$141.2x800x1.25x\left(\frac{0.29}{10}\right) = 4095 \text{ md ft } (1.23\mu m^3)$$

The time match was used to compute the wellbore storage coefficient (for $C_De^{2S} = 10$, no unit slope log-log straight line is available) :

$$C = \frac{kh}{3389}\left(\frac{\Delta t}{t_D/C_D}\right)_{match} = \frac{4095}{3389}\left(\frac{0.1}{0.48}\right) = 0.25 \text{ bbl/psi}$$
$$(5.8\ 10^{-6}\text{m Pa}^{-1})$$

which is much greater than that computed from well completion data. The dimensionless wellbore constant is calculated as :

$$C_D = \frac{0.8936C}{\phi\mu C_t hr_w^2} = \frac{0.8936x0.25}{0.15x1x16.10^{-6}x30x(0.3)^2} = 34475$$

The skin can then be obtained from the curve match :

$$S = 0.5 \ln\left[\frac{(C_De^{2S})_{match}}{C_D}\right] = 0.5\ln\left(\frac{10}{34475}\right) = -4$$

This last result indicates a highly stimulated well, which is not consistent with the curve match. Proceeding further, MDH and Horner plots were made as shown on Fig. 16. Straight lines can be clearly identified on both plots, but slopes are different (respectively, 38 and 71.5 psi/log ∞). The MDH analysis yields :

$$kh = 162.6\frac{qB\mu}{m} = 162.6\frac{800x1.25x1}{38} = 4279 \text{ md ft } (1.29\mu m^3)$$

$$S = 1.151\left[\frac{\Delta p_{1hr}}{m} - \log\frac{kh}{\phi c_t \mu hr_w^2} + 3.23\right]$$

$$= 1.151\left[\frac{81}{38} - \log\frac{4279}{0.15x1x16.10^{-6}x30x(0.3)^2} + 3.23\right] = -4$$

$$p_i = p_{ws}(\Delta t=0) + \Delta p_{1hr} + m\log t_p = 81 + 38\log(22.45)$$

$$= 3230 \text{ psi } (222.710^5 \text{ Pa})$$

while Horner analysis results are :

$$kh = 162.6\frac{800x1.25x1}{71.5} = 2274 \text{ md ft } (0.68\mu m^3)$$

$$S = 1.151\left[\frac{3155 - 3097}{71.5} - \log\frac{2274}{0.15x1x16.10^{-6}x30x(0.3)^2} + 3.23\right] = -5.0$$

$$p_i = 3253 \text{ psi } (234.3\ 10^5 \text{ Pa})$$

MDH results are consistent with the log-log analysis, but not those from Horner analysis. Another puzzling finding is that a drawdown log-log plot --$p_i - p_{wf}$ vs production time-- with the MDH p_i does not coincide with the build-up one, even at early times. On the other hand, a good early time agreement is obtained between drawdown (triangles in Figs 15 and 16) and build-up on the log-log graph when the Horner p_i is used for calculating the drawdown pressure drop. The two curves depart at long times, with the build-up curve falling below the drawdown curve, which is typical of too short a production period. This is confirmed by plotting the build-up data as $(p_{wo} - p_{wf,ext})$ vs Δt (squares in Figs 15 and 16) : the resulting curve matches perfectly the drawdown curve corresponding to the Horner p_i.

The drawdown period was thus too short for the build-up to be analyzed with a drawdown type-curve. This could have been realized by checking the minimum drawdown duration required for the build-up log-log match with $C_De^{2S} = 10$ to be valid. Matching the last measured build-up point ($\Delta t = 71$ hrs) would require :

$$\frac{\Delta t}{t_p} < 0.5$$

or $t_p > 142$ hrs, compared to an actual production time of 24.5 hrs. The match is therefore not correct. The last build-up point that can be matched on a

drawdown curve in that C_De^{2S} region must correspond to $\Delta t < 12$ hrs. As pointed out in a previous chapter, a new match must be attempted with a lower C_De^{2S} value, with the build-up points after 12 hrs falling below the matched type-curve. The result is shown in Fig. 15, where a perfect match is obtained with $C_De^{2S} = 1$, which indicates an acidized or slightly fractured well. Quantitative log-log analysis then yields :

match point : $p_D = 0.16$; $\frac{t_D}{C_D} = 0.35$ /$\Delta p=10$; $\Delta t=0.1$

pressure match : $kh = 141.2 \times 800 \times 1.25 \times 1 \times \frac{0.16}{10} = 2259$ md ft

time match : $C = \frac{2259}{3389} \frac{0.1}{0.35} = 0.19$ bbl/psi

$$C_D = \frac{0.8936 \times 0.19}{0.15 \times 1 \times 16.10^{-6} \times 30 \times (0.3)^2} = 26200$$

curve match : $S = 0.5 \ln\left(\frac{1}{26200}\right) = -5.1$

This is an excellent agreement with the Horner analysis results. The final conclusion was that the reservoir was probably fissured, with natural fractures communicating with the well as a result of acidification. The gross behavior of the reservoir is identical to that of a homogeneous reservoir with one single infinite conductivity vertical fracture, with a fracture half length equal to :

$$x_f = 2\, r_w e^{-S} = 90 \text{ ft } (27\text{m})$$

CONCLUSIONS

In this paper , we have discussed the relationship between the so-called "conventional" and "modern" analysis methods. It has been shown that "conventional" methods constitue a small sub-set of the techniques available for interpretation, and therefore provide only limited results, compared to what can be obtained with all the different methods specific to the various flow regimes identified on the test data.

It was pointed out that, although they are commonly both referred to as "conventional", the Miller Dyes Hutchinson and the Horner methods are essentially different. The MDH method is a particular application of log-log analysis, and is only valid for build-up data when type-curve matching with drawdown type-curves is justified. It is also required that the match be in the portion of the drawdown type-curve where the semi-log approximation applies.

When build-up data are plotted as $\log [p_{ws}(\Delta t) - p_{ws}(\Delta t=0)]$ versus $\log \Delta t$, the validity of log-log analysis with drawdown type-curves depends upon the relative duration of the build-up and the drawdown periods : for stimulated wells, the production time must be greater than the longest build-up time, whereas it may be shorter for damaged wells. On the other hand, build-up log-log analysis with drawdown type-curves is always valid when shut-in pressures are plotted as $\log [p_{ws}(\Delta t) - p_{wf,ext}(\Delta t)]$ versus Δt, where $p_{wf,ext}$ is the extrapolated drawdown pressure. This last plot should be used instead of the previous one whenever possible.

A new type-curve was introduced for analyzing tests where early time data are dominated by wellbore storage. This type-curve is applicable to fractured and non-fractured wells and includes realistic time limits for the various dominating flow regimes, as an aid to log-log analysis. This new type-curve covers a wider range of well conditions than the ones available in the literature and was found to be more efficient as a qualitative and quantitative interpretation tool, when wellbore storage does not change during the test.

ACKNOWLEDGEMENT

The authors are grateful to the management of FLOPETROL for permission to publish this paper.

NOMENCLATURE

- A = drainage area, sq.ft
- B = formation volume factor, RB/STB
- c_t = system total compressibility, psi^{-1}
- C = wellbore storage, Bbl/psi
- C_D = dimensionless storage constant
- C_{Df} = wellbore storage for a fractured well
- h = formation thickness, ft
- k = permeability, millidarcies
- k_f = fracture permeability, millidarcies
- $k_{fD}w_{fD}$ = dimensionless fracture conductivity
- m = ± slope of linear portion of semilog plot of pressure transient data, psi/cycle
- p = pressure, psi; Laplace transformed variable
- $\bar{p}$ = volumetric average pressure within drainage region resulting from constant-rate production for a time t
- p_D = dimensionless pressure
- p_i = initial reservoir pressure, or stabilized pressure at start of test, psi
- p_{1hr} = pressure on straight-line portion of Horner semilog plot 1 hour after beginning a transient test
- p_{wf} = flowing bottom-hole pressure, psi
- Δp = pressure change, psi
- q = flow rate, STB/D
- r_e = distance to constant pressure boundary
- r_f = horizontal fracture radius, ft
- r_w = wellbore radius, ft
- r_{we} = apparent or effective wellbore radius (includes effects of wellbore damage or improvement), ft
- S = van Everdingen-Hurst skin factor
- t = time, hours
- t_D = dimensionless time
- t_{Df} = dimensionless time based on half fracture length of a vertical fracture
- t_{DA} = dimensionless time based on drainage area
- t_p = production time, hrs
- Δt = elapsed time, hrs
- x_f = vertical fracture length from center of well to tip of fracture, ft

w = fracture width, ft
μ = viscosity, cp
ϕ = porosity, fraction

SUBSCRIPTS

A = based on drainage area A
D = dimensionless
e = effective; outer boundary
f = fracture; flowing
i = initial
r = radial dimension
s = static (zero surface production rate)
w = bottom hole, well
z = vertical dimension

REFERENCES

1. Ramey, H.J., Jr. :"Short-Time Well Test Data Interpretation in the Presence of Skin Effect and Wellbore Storage," J. Pet Tech. (Jan 1970) 97.
2. Earlougher, R.C., Jr. and Kersch, K.M. : "Analysis of Short-Time Transient Test Data by Type-Curve Matching," J. Pet. Tech. (July1974) 793.
3. Ramey, H.J.,Jr. : "Practical Use of Modern Well Test Analysis", paper SPE 5878, presented at the SPE-AIME 46th Annual California Regional Meeting, Long Beach, April 7-9, 1976.
4. Horner, D.R. : "Pressure Build-Up in Wells," Proc., Third World Pet. Cong., E.J. Brill, Leiden (1951) II, 503-521.
5. Miller, C.C., Dyes, A.B., and Hutchinson, C.A., Jr. : "Estimation of Permeability and Reservoir Pressure from Bottom-Hole Pressure Build-up Characteristics," Trans., AIME (1950) 189, 91-104.
6. Theis, C.V. : "The Relationship between the Lowering of the Piezometric Surface and the Rate and Duration of Discharge Using Ground-Water Storage," Trans., AGU (1935) 519.
7. Gringarten, A.C., Ramey, H.J., Jr., and Raghavan, R. : "Applied Pressure Analysis for fractured Wells," J. Pet. Tech. (July 1975) 887-892.
8. Cinco L., H., and Samaniego V., F. : "Transient Pressure Analysis for Fractured Wells", paper SPE 7490, presented at the SPE-AIME 53rd Annual Fall Technical Conference and Exhibition, Houston, Texas, Oct 1-3, 1978.
9. van Everdingen, A.F., and Hurst, W. : "The Application of the Laplace Transformation to Flow Problems in Reservoirs," Trans., AIME (1949) 186, 305-324.
10. Moran, J.H., and Finklea, E.E. : "Theoretical Analysis of Pressure Phenomena Associated with the Wireline Formation Tester", J. Pet. Tech. (Aug. 1962) 899.
11. Jones, P. : "Reservoir Limit Tests", Oil and Gas J. (June 18, 1956) 54, N° 59,184
12. Raghavan, R., Cady, G.V. and Ramey, H.J., Jr. : "Well-Test Analysis for Vertically Fractured Wells", J. Pet. Tech. (Aug. 1972) 1014.
13. Gringarten, A.C. and Ramey, H.J., Jr. : "Unsteady - State Pressure Distributions Created by a Well With a Single Horizontal Fracture, Partial Penetration, or Restricted Entry", Soc. Pet. Eng. J. (Aug. 1974) 347.
14. Cinco L., H., Samaniego V., F., and Dominguez A., N. : "Transient Pressure Behavior for a Well With a Finite-Conductivity Vertical Fracture", Soc. Pet. Eng. J. (Aug. 1978) 253.
15. Cinco L., H. : private communication.
16. Agarwal, R.G., Al-Hussainy, R., and Ramey, H.J., Jr. : "An investigation of Wellbore Storage and Skin Effect in Unsteady Liquid Flow. I : Analytical Treatment," Soc. Pet. Eng. J. (Sept. 1970) 279.
17. McKinley, R.M. : "Wellbore Transmissibility from Afterflow-Dominated Pressure Buildup Data," J. Pet. Tech. (July 1971)
18. Ramey, H.J., Jr., and Gringarten, A.C. : "Effect of High Volume Vertical Fractures on Geothermal Steam Well Behavior," Proceedings, 2nd United Nations Symposium on the Use and Development of Geothermal Energy, San Francisco, Ca., May 20-29, 1975.
19. Cinco L., H. and Samaniego, F. : "Effect of Wellbore Storage and Damage on the Transient Pressure Behavior of Vertically Fractured Wells", paper SPE 6752, presented at the 52nd Annual Technical Conference and Exhibition of SPE of AIME, Denver, Colorado, Oct 9-12, 1977.
20. Ramey, H.J., Jr., Kumar, A., and Gulati, M.S. : "Gas Well Test Analysis under Water-Drive Conditions, American Gas Association Monograph, 1973.
21. Chen, H.K. and Brigham, W.E. : "Pressure Build-up for a Well With Storage and Skin in a Closed Square", J. Pet. Tech. (Jan. 1978) 141.
22. Raghavan, R. : "The Effect of Producing Time on Type-Curve Analysis", submitted for publication to the Society of Petroleum Engineers.
23. Ramey, Henry J., Jr., and Cobb, W.M. : "A General Pressure Build-up Theory for a Well in a Closed Drainage Area," J. Pet. Tech. (December 1971) 1493.
24. Ramey, H.J., Jr. : "Interference Analysis for Anisotropic Formations.. A Case History". J. Pet. Tech. (Oct. 1975) 1290.
25. Slider, H.C. : "A Simplified Method of Pressure Build-up Analysis for a Stabilized Well", J. Pet. Tech. (Sept. 1971) 1155.
26. Odeh, A.S. and Jones, L.G. :"Pressure Drawdown Analysis, Variable Rate Case", J. Pet. Tech. (Aug. 1965) 960.
27. de França C., A.C. : "A Study of the Pressure Behavior of Circular Reservoirs", Master of Science Thesis, Stanford University, Stanford, May 1978.

TABLE 1

DATA FOR EXAMPLE TEST

$h = 30$ ft
$B = 1.25$ RB/STB
$\mu = 1.0$ cp
$\phi = 0.15$
$c_t = 10\ 10^{-6}$ psi $^{-1}$
$q = 800$ bbl/D
$r_w = 0.3$ ft

DRAWDOWN			BUILD-UP				
Δt (mn)	p_{wf} (psi)	$p_{wf}(\Delta t=0)-p_{wf}(\Delta t)$ (psi)	Δt (min)	p_{ws} (psi)	$p_{ws}(\Delta t)-p_{ws}(\Delta t=0)$ (psi)	$p_{ws}(\Delta t)-p_{wf,ext}(\Delta t)$ (psi)	$\frac{t_p+\Delta t}{\Delta t}$
45	3198	55	3	3105	8	9	451.2
85	3180	73	5	3108	11	12	300.5
192	3154	99	9	3115	18	19	155.9
297	3141	112	16	3125	28	29	86.3
417	3130	123	30	3139	42	44	45.3
654	3116	137	40	3146	49	50	34.9
983	3106	147	66	3159	62	64	21.5
1347	3097	156	100	3171	74	77	14.5
			138	3180	83	86	10.8
			252	3195	98	104	6.4
			334	3203	106	113	5.0
			423	3208	111	119	4.2
			574	3216	119	130	3.4
			779	3222	125	139	2.7
			1092	3228	131	149	2.2
			1674	3234	137	161	1.8
			2186	3238	141	170	1.6
			2683	3242	145	178	1.5
			3615	3246	149	188	1.4
			4281	3246	149	191	1.3

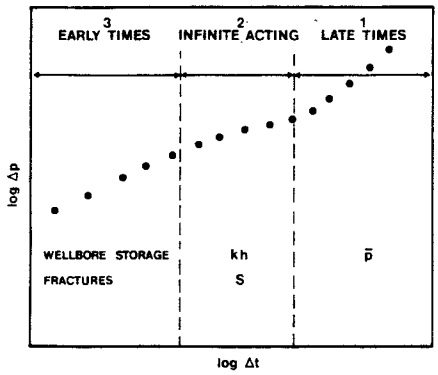

Fig. 1 - Schematic log-log plot of a typical test.

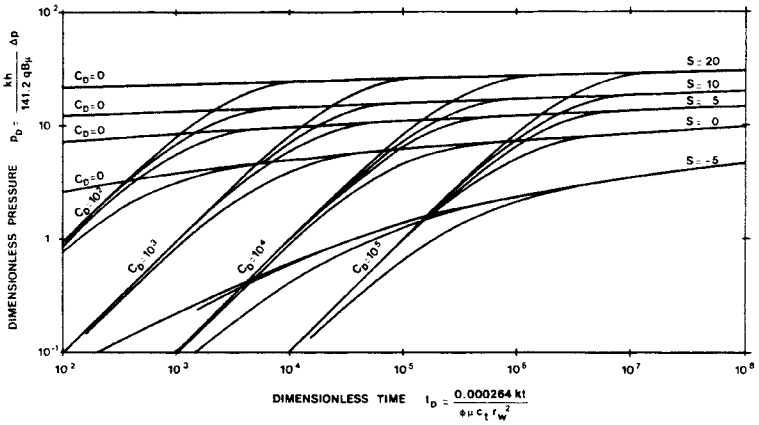

Fig. 2 - Agarwal, Al-Hussainy and Ramey type-curve (ref. 16).

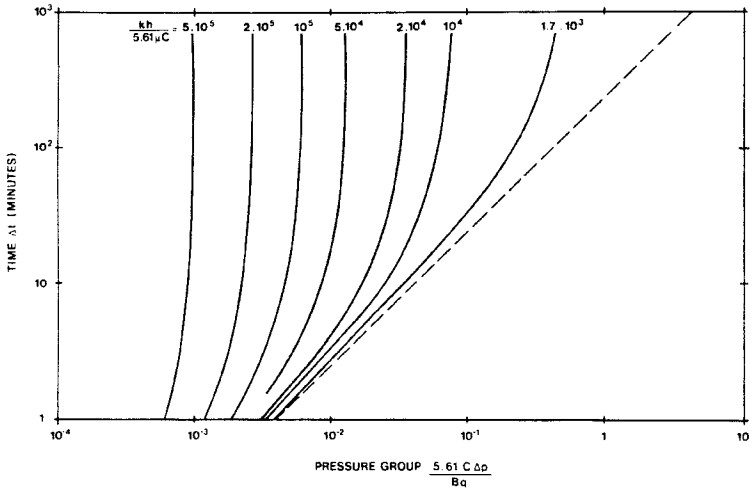

Fig. 3 - McKinley type-curve (ref.17).

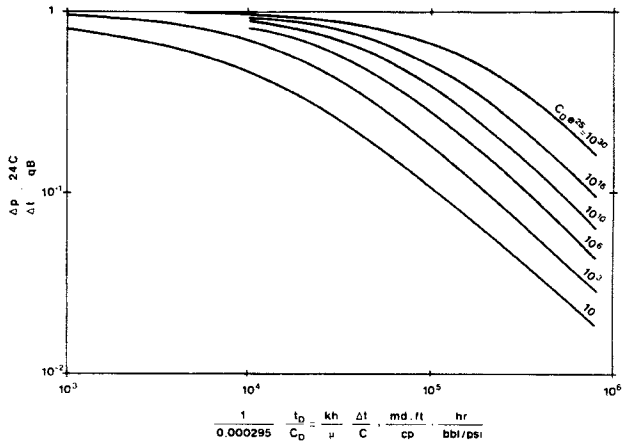

Fig. 4 - Earlougher and Kersch type-curve (ref. 2).

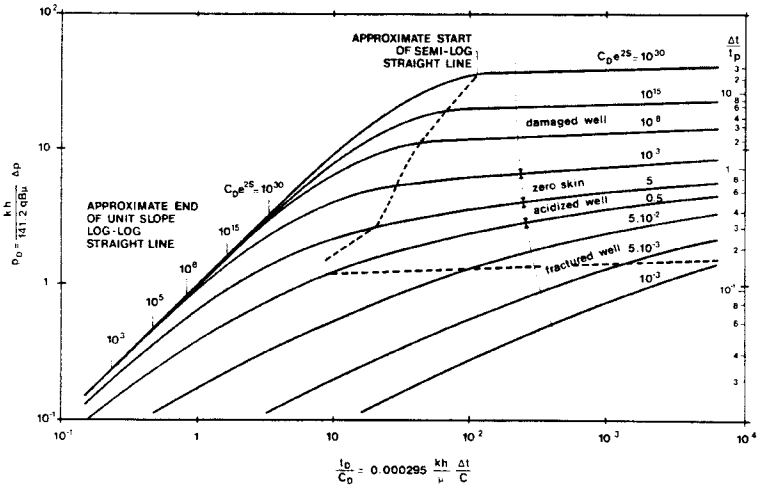

Fig. 5 - New type-curve for wellbore storage and skin effects (by permission of Flopetrol).

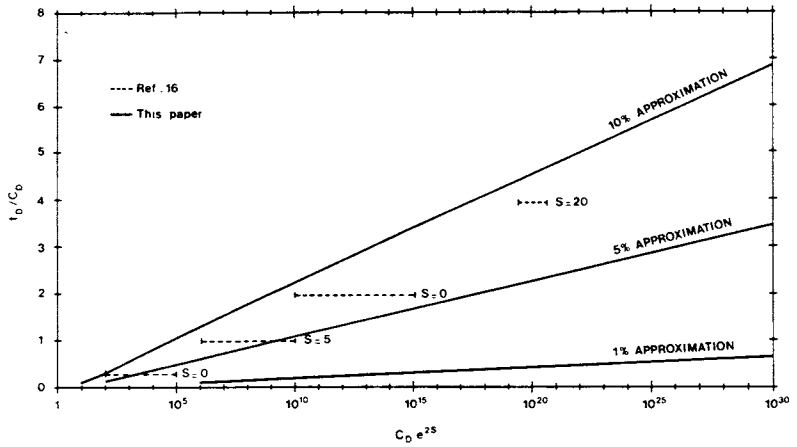

Fig. 6 - Dimensionless time at approximate end of unit slope.

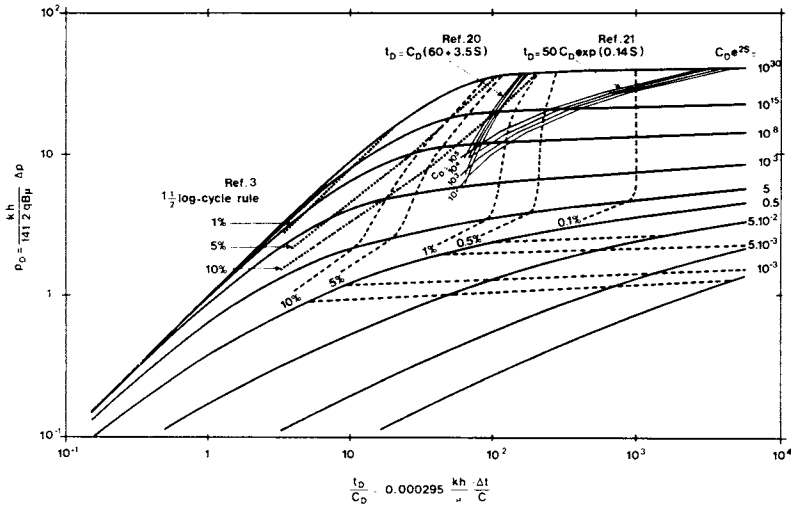

Fig. 7 - A comparison between different approximation criteria for the start of the semi-log straight line.

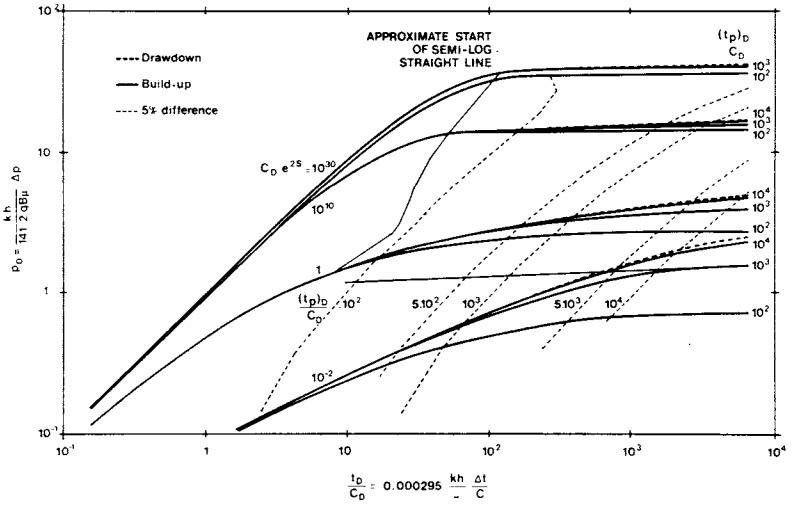

Fig. 8 - Build-up type-curve for a well with wellbore storage and skin effects.

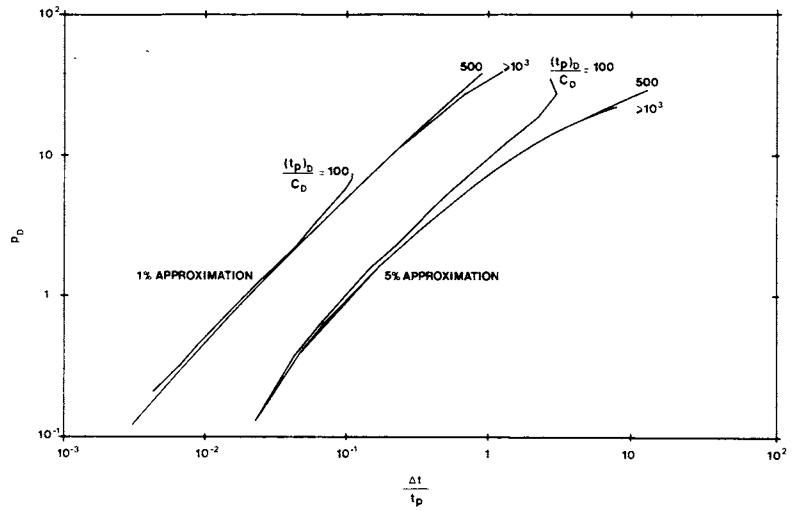

Fig. 9 - End of validity of build-up log-log analysis with drawdown type-curve.

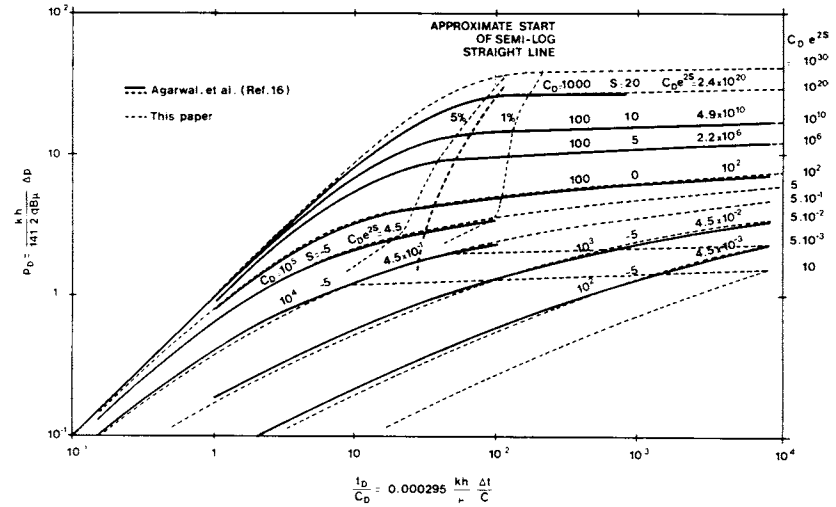

Fig. 10 - Comparison between type-curves from Figs 2 and 5.

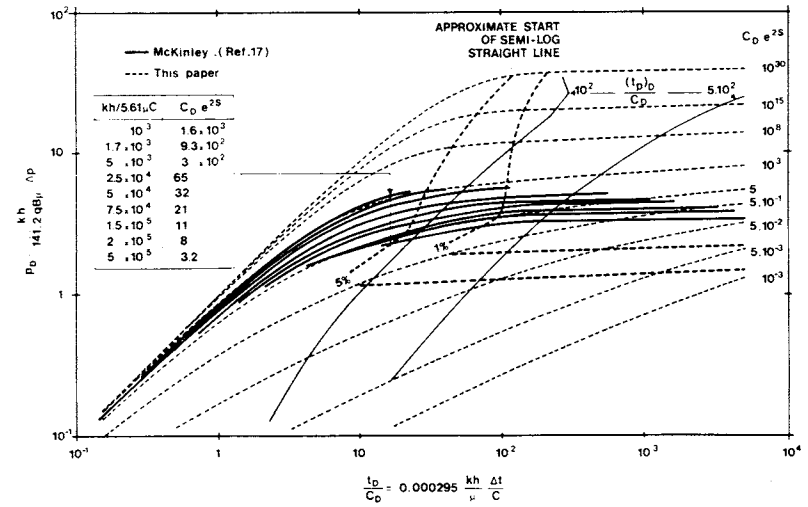

Fig. 11 - Comparison between type-curves from Figs 3 and 5.

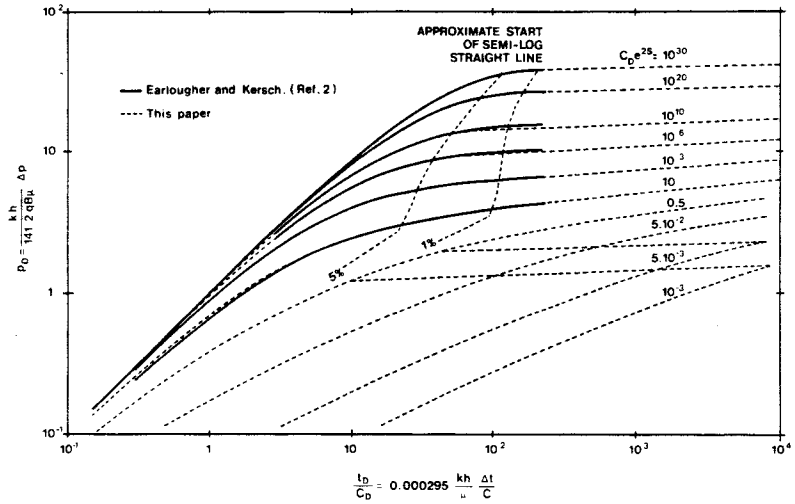

Fig. 12 - Comparison between type-curves from Figs 4 and 5.

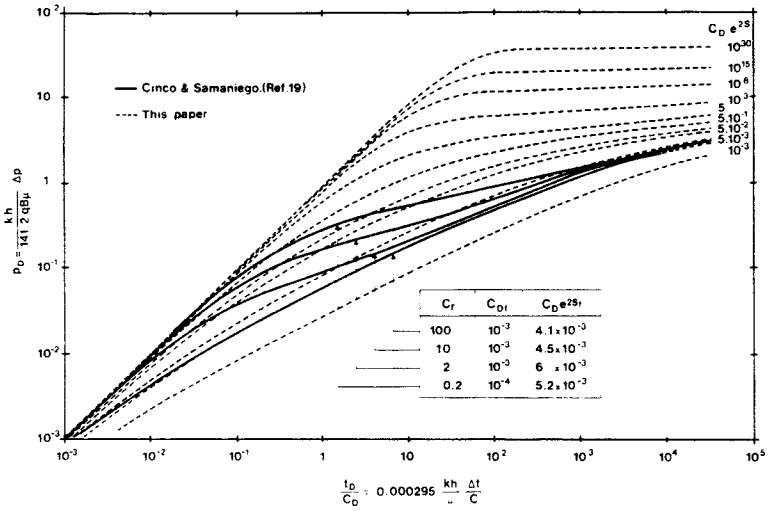

Fig. 13 - Comparison between the type-curve of Fig. 5 and the type-curve for a finite conductivity well with wellbore storage (ref 19).

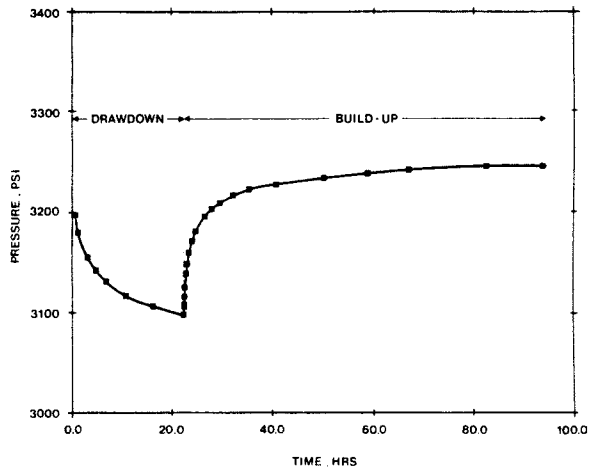

Fig. 14 - Example test.

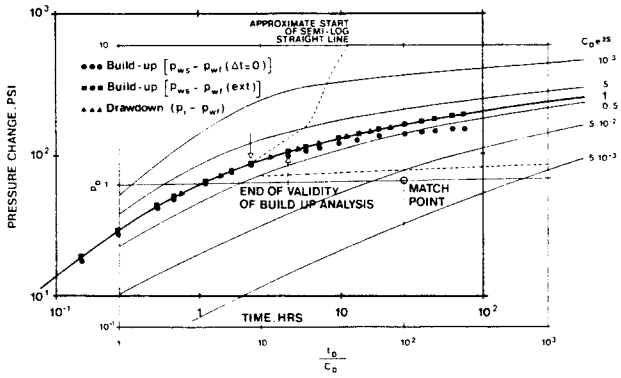

Fig. 15 - Log-log analysis of example test.

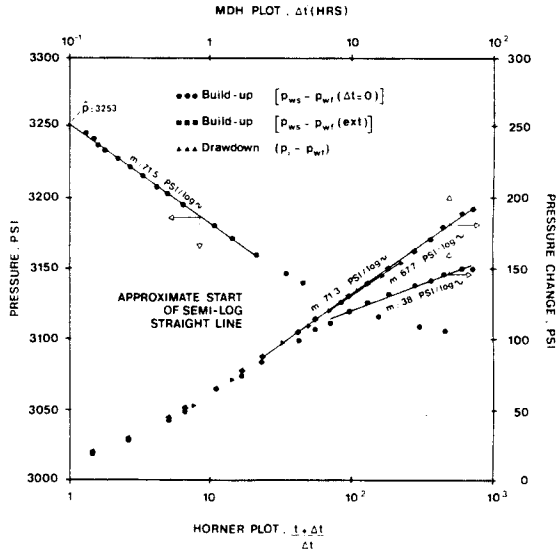

Fig. 16 - Semi-log analysis of example test.